Dynamics of stromelysin/inhibitor interactions studied by ^{15}N NMR relaxation measurements: Comparison of ligand binding to the S_1-S_3 and S'_1-S'_3 subsites

Peng Yuan[a,*], Vincent P. Marshall[b], Gary L. Petzold[b], Roger A. Poorman[b] & Brian J. Stockman[a,**]

[a]*Structural, Analytical and Medicinal Chemistry and* [b]*Protein Science, Pharmacia & Upjohn, 301 Henrietta St., Kalamazoo, MI 49001, U.S.A.;* *Present address: Pharmacy Department, Warren G. Magnuson Clinical Center, National Institutes of Health, Bethesda, MD 20892, U.S.A.*

Abstract

This report describes the backbone amide dynamics of the uniformly ^{15}N labeled catalytic domain of human stromelysin complexed to PNU-99533, a hydroxamate-containing ligand that binds to the S'_1-S'_3 region (right side) of the stromelysin active site, and to PNU-107859 and PNU-142372, both thiadiazole-containing ligands that bind to the S_1-S_3 region (left side) of the stromelysin active site. ^{15}N R_1, R_2 and NOE NMR relaxation measurements were recorded and analyzed for each complex. Different dynamic behaviors were observed for stromelysin complexed to the two classes of ligands, indicating that it may be possible to use protein dynamics to distinguish between different binding orientations. In the absence of bound ligand at the S_1-S_3 subsites, the S_1-S_3 residues were found to be relatively rigid. In contrast, the S'_1-S'_3 subsites were found to be flexible in the absence of interactions with ligand. The relative rigidity of the S_1-S_3 subsites may be responsible for MMP binding specificity by discriminating between ligands of different shapes. By contrast, the inherent flexibility of the S'_1-S'_3 subsites allows structural rearrangement to accommodate a broad range of incoming substrates or inhibitors. Similarities and differences in dynamics observed for each complex provide insights into the interactions responsible for protein–ligand recognition. The relevance of protein dynamics to structure-based drug design is discussed.

Introduction

Matrix metalloproteinases (MMPs), including stromelysin, are a family of zinc-containing endopeptidases that function in tissue remodeling processes. These peptidases collectively degrade the protein components of connective tissue and are generally regulated by selective endogenous tissue inhibitors of metalloproteinases (TIMPs) (Wojtowicz-Praga et al., 1997). Overexpression of the MMPs, or reduced levels of TIMPs, has been implicated in a number of disease states such as arthritis, cancer metastasis and related connective tissue disorders (MacDougall and Matrisian, 1995; Cawston, 1996). The catalytic domain of human stromelysin (referred to as stromelysin throughout the text) has been used as a target enzyme in the discovery of potent inhibitors which may have therapeutic value in the treatment of the above mentioned diseases. This 20 kDa domain has similar kinetic, catalytic and inhibitory properties as full
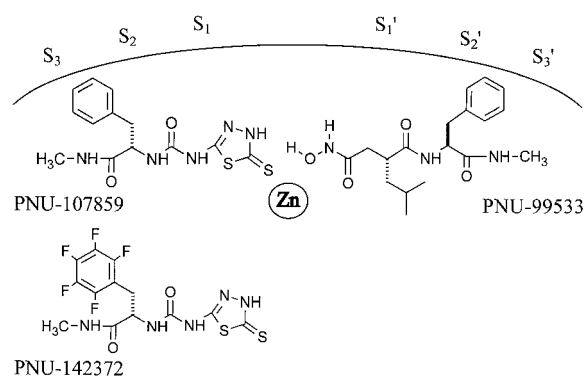

Figure 1. Schematic of the stromelysin active site indicating the binding orientations of the hydroxamate (PNU-99533) and thiadiazole (PNU-107859 and PNU-142372) ligands.

length stromelysin, a 45 kDa protein, and is a suitable target for structure-based drug design.

The three-dimensional structures of stromelysin complexed with a number of inhibitors have been reported (Gooley et al., 1993, 1994, 1996; Van Doren et al., 1993, 1995; Becker et al., 1995; Dhanaraj et al., 1996; Finzel et al., 1998; Stockman et al., 1998). The global fold consists of three α-helices and a five-stranded β-sheet composed of four parallel strands and one anti-parallel strand. The active site is a cleft spanning the width of the enzyme containing a catalytic zinc atom in the center coordinated by three histidine residues. Several classes of MMP inhibitors have been discovered. The most common contain a zinc-ligating hydroxamic acid, carboxylic acid or thiol group attached to a small peptide fragment capable of binding to specificity pockets of the MMP enzymes (Porter et al., 1995; Zask et al., 1996). As shown schematically in Figure 1, ligands coordinate the catalytic zinc atom and interact with either the S_1-S_3 or S'_1-S'_3 subsites. The vast majority of inhibitors described to date bind in an extended conformation in the right side (S'_1-S'_3) of the active site of the protein as exemplified here by PNU-99533. Recently, the thiadiazole class of inhibitor was discovered and determined to interact with the left side (S_1-S_3) of the active site as exemplified by PNU-107859 and PNU-142372 (Finzel et al., 1998; Stockman et al., 1998; Jacobsen et al., 1999). The availability of two classes of ligands that bind in distinctly different manners to stromelysin provides an opportunity to investigate the role that protein dynamics plays in stromelysin/ligand molecular recognition interactions.

It has become clear in recent years that highly specific molecular recognition processes that occur in biological systems are intimately dependent on the dynamic properties of the species involved. Understanding the nature of the motions demonstrated by these species will undoubtedly help in the design of specific inhibitors of protein function. By examining the motional properties of a free and ligated protein, the role that dynamics plays in ligand recognition can be assessed. We have studied the protein dynamics of a number of stromelysin/ligand complexes. In these studies, relaxation rates of backbone amide ^{15}N nuclei were measured and motional parameters were extracted from the relaxation rates using the model-free formalism of Lipari and Szabo (1982a, b). The dynamics of stromelysin complexed with PNU-99533, PNU-107859 and PNU-142372 are presented here. Different dynamic behaviors were observed for stromelysin complexed with different types of ligands, thus distinguishing binding location and orientation. Such differences are critical in evaluating key stromelysin–ligand interactions as well as the local and global impact of ligand binding. The relevance of protein dynamics to structure-based drug design of MMP inhibitors will be discussed in this context.

Materials and methods

Sample preparation

The catalytic domain of stromelysin, consisting of residues 83–255, was prepared as described previously (Stockman et al., 1998). PNU-99533 (Dickens et al., 1987), PNU-107859 (Jacobsen et al., 1999) and PNU-142372 (Jacobsen et al., 1999) were synthesized as described previously. The stromelysin/ligand complexes were prepared by first dissolving a small amount of ligand in [^{2}H$_6$]DMSO and then adding between 5–10 μl of this solution to the aqueous protein sample. The NMR samples contained 0.9 mM [^{15}N]stromelysin dissolved in 10 mM [^{2}H$_4$]imidazole buffer, 2.5 mM CaCl$_2$ and 5 μM ZnCl$_2$ at pH 6.5. Samples contained a slight excess of ligand to protein.

NMR spectroscopy

NMR spectra were acquired at 300 K on a Bruker AMX-600 NMR spectrometer equipped with a triple-resonance, pulse field gradient probe with actively shielded 3-axis gradients and a gradient amplifier unit. The pulse sequences used to record ^{15}N R_1, R_2 and steady-state ^{15}N{^{1}H} NOE spectra were those described by Barbato et al. (1992), modified to include

pulse field gradients (Bax and Pochapsky, 1992) for artifact elimination, coherence selection and solvent suppression. A combination of water flip-back (Grzesiek and Bax, 1993) and WATERGATE (Piotto et al., 1992) techniques were used in the NOE measurements, while only WATERGATE was used in R_1 and R_2 measurements to eliminate the water resonance. WALTZ-16 decoupling (Shaka et al., 1983) was used to decouple ^{15}N during acquisition in all experiments.

For ^{15}N R_1 measurements of the stromelysin/PNU-99533 complex, 32 scans were acquired for each t_1 increment. A 100×1024 real data matrix was acquired for nine different durations of the R_1 relaxation delay: 32, 128, 256, 384, 512, 768, 1024, 1536 and 2048 ms. A 4 s relaxation delay was used between scans. The same parameters were used for the stromelysin/PNU-107859 complex, except that 10 relaxation delays were collected: 32, 128, 256, 384, 512, 768, 1024, 1280, 1536 and 2048 ms, and for the stromelysin/PNU-142372 complex except that 11 relaxation delays were collected: 32, 64, 128, 256, 354, 512, 640, 832, 1024, 1536 and 2048 ms.

For ^{15}N R_2 measurements of the stromelysin/PNU-99533 complex, the same number of scans and data matrix sizes as with the R_1 data were acquired, but with seven different R_2 relaxation delays: 8, 32, 64, 96, 128, 160 and 196 ms. A 2 s relaxation delay was used between scans. The same parameters were used for the stromelysin/PNU-107859 complex, except that eight relaxation delays were collected: 8, 32, 64, 96, 128, 160, 192 and 256 ms, and for the stromelysin/PNU-142372 complex, except that the eight relaxation delays used were: 8, 16, 32, 48, 64, 96, 128 and 192 ms. Both the R_1 and R_2 experiments were recorded with magnetization relaxing as a single exponential decay and in such a way that the delays between scans affected only the sensitivity and not the extracted relaxation rates (Sklenar et al., 1987).

The steady-state ^{15}N{^{1}H} NOE of each complex was recorded with a 256×1024 real data matrix and 64 scans. Non-selective ^{1}H saturation was achieved with the use of ^{1}H pulses applied every 15 ms for a period of 3 s. In the case of the no-NOE spectra, a relaxation delay of 5 s was employed, while a relaxation delay of 2 s prior to the 3 s ^{1}H presaturation period was employed for the NOE spectra.

The R_1, R_2 and NOE data sets were processed using Lorentzian-to-Gaussian filtering functions in both dimensions. Zero filling to 1024 and 2048 data points was used in the t_1 and t_2 dimensions, respectively. The data were processed and analyzed using NMR-Pipe, NMRDraw and NMRCompass from Molecular Simulations, Inc. Resonance intensities rather than integrated peak volumes were used to determine relaxation rates because accurate integration requires well-separated resonances.

Analysis of relaxation data

Relaxation of an amide ^{15}N nucleus spin at high magnetic field is dominated by the dipolar interaction with the directly attached proton spin and by chemical shift anisotropy as described by Abragam (1961). Processes other than dipole-dipole and chemical shift anisotropy that contribute to the decay of transverse magnetization are included in an R_{ex} term (Bloom et al., 1965). In many cases, these contributions are the result of conformational exchange averaging. Conformational exchange processes represented by R_{ex} will be referred to here as dynamics on a μs–ms time scale.

Analysis of R_1, R_2 and NOE data followed the procedure outlined by Mandel et al. (1995). The relaxation rates were analyzed using the model-free formalism proposed by Lipari and Szabo (1982a, b) and extended by Clore et al. (1990). The spectral density function, $J(\omega)$, is modeled as (Clore et al., 1990; Mandel et al., 1995)

$$J(\omega) = \frac{2}{5}\left[\frac{S^2\tau_m}{1+(\omega\tau_m)^2} + \frac{(1-S_f^2)\tau_f'}{1+(\omega\tau_f')^2} + \frac{(S_f^2-S^2)\tau_s'}{1+(\omega\tau_s')^2} \right]$$

where $\tau_f' = \tau_f\tau_m/(\tau_f+\tau_m)$, $\tau_s' = \tau_s\tau_m/(\tau_s+\tau_m)$, τ_m is the overall rotational correlation time of the molecule, τ_f is the effective correlation time for internal motion on a fast time scale ($\tau_f < 100$ to 200 ps), τ_s is the effective correlation time for internal motions on a slow time scale ($\tau_f < \tau_s < \tau_m$), $S^2 = S_f^2 S_s^2$ is the generalized order parameter characterizing the amplitude of the internal motions, and S_f^2 and S_s^2 are the order parameters for the internal motions on the fast and slow time scales, respectively. The order parameters specify the degree of spatial restriction of the ^{1}H-^{15}N bond vector, with values ranging from zero for isotropic internal motions to unity for completely restricted motion, and represent dynamics on the ps–ns time scale.

Since a minimum of six parameters would be needed to fully describe the dynamics of a specific ^{1}H-^{15}N bond vector but only three relaxation parameters are measured, five simpler models were used to fit the experimental data (Mandel et al., 1995). Each model contains an overall rotational correlation time, a

maximum of three internal motional parameters and at most a single internal time scale parameter, either τ_f or τ_s. In these models, the internal time scale parameter will be referred to as τ_e. The five models consisted of the following subsets of the extended model-free parameters: (1) S^2; (2) S^2, $\tau_e = \tau_f$; (3) S^2, R_{ex}; (4) S^2, $\tau_e = \tau_f$, R_{ex}; (5) S^2, S_f^2, $\tau_e = \tau_s$.

Model-free parameters were determined from the relaxation data with selected models by using the FORTRAN program Modelfree v. 3.1 (Palmer et al., 1991). An initial estimate of the overall rotational correlation time, τ_m, was obtained from the 10% trimmed mean of the R_2/R_1 ratio for the backbone amide resonances (Kay et al., 1989). A grid search was used to obtain initial guesses for the values of the other parameters. A complete description of model selection used in data analysis can be found in Mandel et al. (1995).

Relaxation data for each stromelysin/ligand complex was analyzed with the assumption that the overall molecular rotational diffusion is isotropic. This assumption was validated by measuring the dimensions of the stromelysin/ligand complexes. All three complexes can be described as having slightly oblate ellipsoid shapes. Their rotational diffusion should not deviate significantly from the isotropic motion of a completely spherical molecule.

Results

Relaxation parameters

Backbone amide chemical shifts of the stromelysin/ PNU-107859 and stromelysin/PNU-142372 complexes were assigned as described previously (Stockman et al., 1998). Assignments for the stromelysin/ PNU-99533 complex were obtained in an analogous fashion and are included here as Supplementary material. Residues 83–90 were not assigned in any complex and are presumed to be disordered in solution. Dynamics measurements were obtained for 138, 141 and 145 backbone amide resonances (out of 159 non-prolyl residues) for the stromelysin/PNU-99533, stromelysin/PNU-107859 and stromelysin/ PNU-142372 complexes, respectively. The unassigned backbone amide resonances appeared as very broad peaks in multi-dimensional spectra, indicative of internal motion and/or rapid exchange with solvent. Values and uncertainties of R_1 and R_2 were determined by non-linear least squares fitting of the experimental data to monoexponential equations using

the method described by Palmer et al. (1991). The rms baseline noise of the spectra was used to estimate peak height uncertainties. Several sets of duplicate spectra were recorded to validate this method. The average uncertainties of R_1 and R_2 over all residues in each complex were 5%. NOE values were calculated as the ratio of the peak intensities measured with and without NOE effects. NOE uncertainties were determined as the standard deviation of the NOE values from replicate measurements and averaged 8% over all residues in each complex. Average R_1, R_2 and NOE values of 1.01 s^{-1}, 15.6 s^{-1} and 0.76, respectively, were obtained for the stromelysin/PNU-99533 complex. Average R_1, R_2 and NOE values of 1.14 s^{-1}, 13.7 s^{-1} and 0.78, respectively, were obtained for the stromelysin/PNU-107859 complex. Average R_1, R_2 and NOE values of 1.12 s^{-1}, 14.2 s^{-1} and 0.77, respectively, were obtained for the stromelysin/PNU-142372 complex. R_1, R_2 and NOE values determined for the three complexes are plotted as a function of residue number in Figure 2.

Motional parameters

The model-free parameters were obtained from fits of the relaxation rates using the methods described above. The average uncertainties are within 5% for most order parameters, but are large for τ_e, and R_{ex}. Values of S^2, τ_e and R_{ex} determined for the three complexes are plotted as a function of residue number in Figure 3. Detailed results for each complex are described below.

Stromelysin/PNU-99533 complex

The overall correlation time of the complex was initially estimated from the R_2/R_1 ratio, 15.23 ± 3.57, to be 12.20 ± 1.57 ns and was determined to be 11.77 ± 0.06 ns from the final analysis. The extracted model-free dynamic parameters are shown in Figure 3. The average S^2 value of the backbone ^{15}N nuclear spins is 0.85. Values of S^2 for the backbone nitrogen atoms have the following distribution: 30 residues have S^2 values less than 0.80, 57 residues have S^2 values between 0.80 and 0.90, and 51 residues have S^2 values greater than 0.90. Only 20 residues required a non-zero τ_e for an adequate fit. Six residues had their τ_e values obtained from the use of model 5, indicating that internal motions associated with these residues are more complicated and flexible, although the validity of these values could not be assessed since R_1, R_2 and NOE were measured at a single field strength only. Seventy-one residues were determined to have
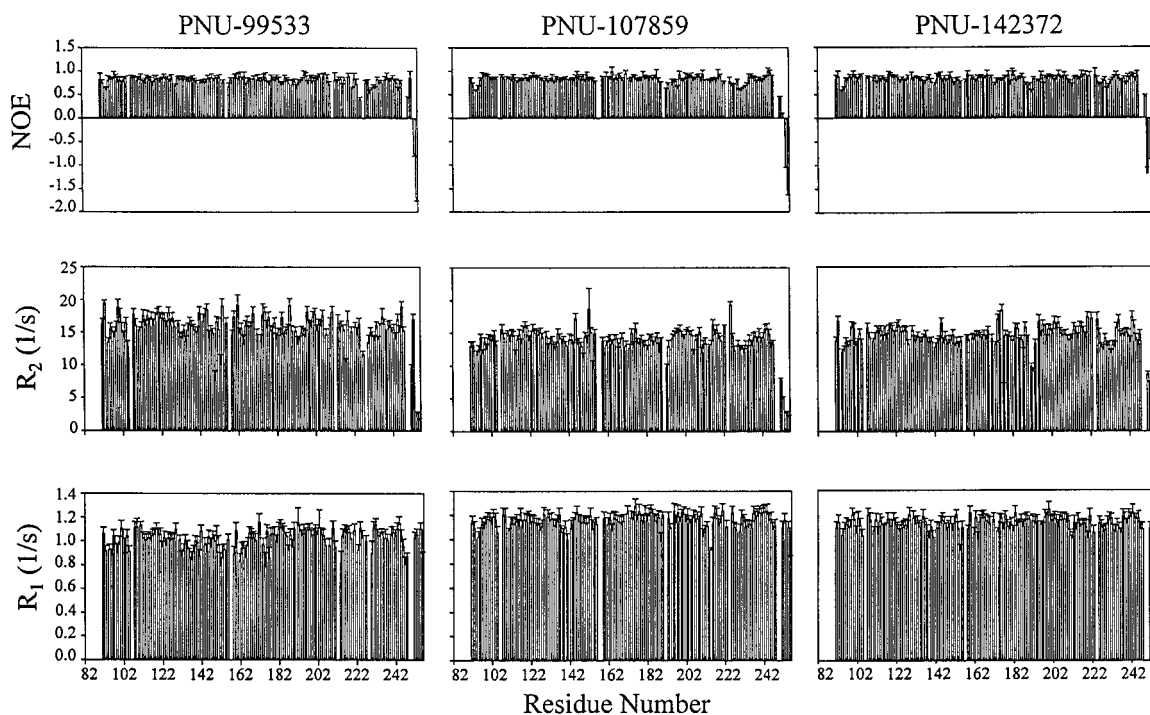
Figure 2. Measured R_1 (bottom row), R_2 (middle row) and NOE (top row) ^{15}N relaxation parameters and their uncertainties plotted as a function of residue number for stromelysin complexed to PNU-99533 (left column), PNU-107859 (middle column) and PNU-142372 (right column). Residues for which no values are shown correspond to either proline residues, unassigned residues or residues for which ^{1}H-^{15}N correlations could not be resolved.

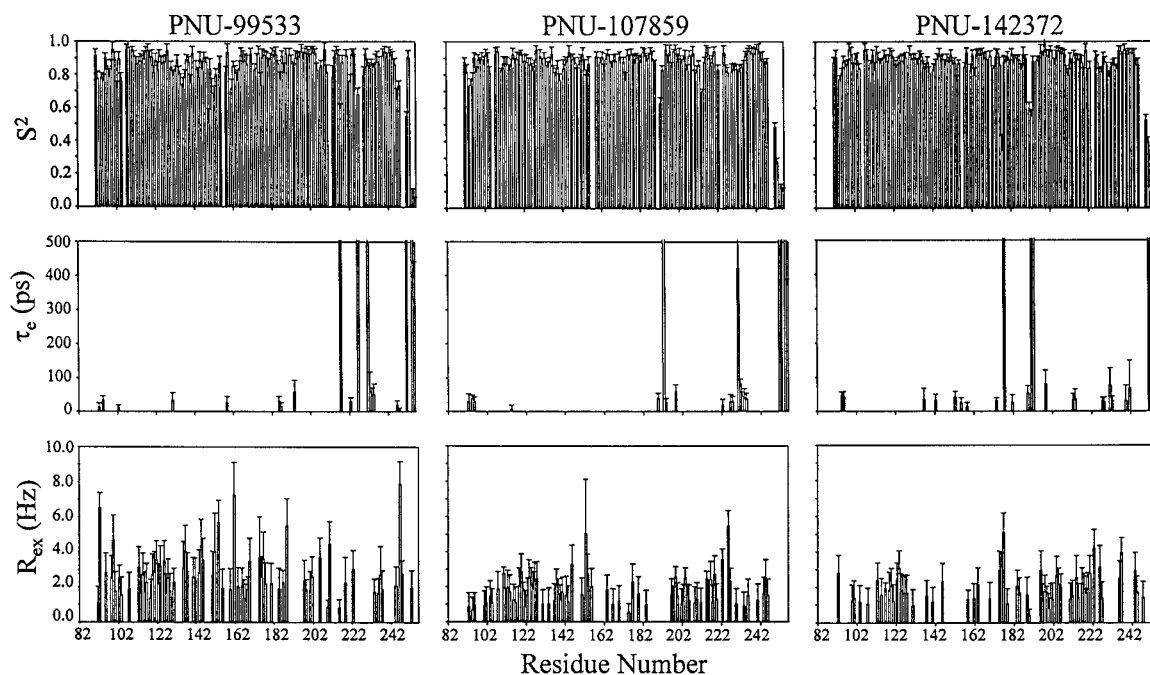*Figure 3.* R_{ex} (bottom row), τ_e (middle row) and S_2 (top row) model-free parameters and their uncertainties plotted as a function of residue number for stromelysin complexed to PNU-99533 (left column), PNU-107859 (middle column) and PNU-142372 (right column).

non-zero R_{ex}, with two of them having R_{ex} values less than 1 s^{-1}. The average R_{ex} value was 2.8 s^{-1}, with 21 residues having R_{ex} values greater than 3 s^{-1}. The results indicate that about one half of the residues are mobile on the μs–ms time scale, resulting from conformational exchange.

Stromelysin/PNU-107859 complex

The overall correlation time of the complex was initially estimated from the R_2/R_1 ratio, 11.95 ± 1.98, to be 10.63 ± 0.98 ns and determined to be 10.43 ± 0.05 ns from the final analysis. The extracted model-free dynamic parameters are shown in Figure 3. The average S^2 value of the backbone ^{15}N nuclear spins is 0.86. Values of S^2 for the backbone nitrogen atoms have the following distribution: 12 residues have S^2 values less than 0.80, 85 residues have S^2 values between 0.80 and 0.90, and 44 residues have S^2 values greater than 0.90. Only 20 residues required a non-zero τ_e for an adequate fit. Six of these had their τ_e values obtained from the use of model 5. Seventy-three residues were determined to have non-zero R_{ex}, with eight of them having R_{ex} values less than 1 s^{-1}. The mean R_{ex} value is 1.7 s^{-1}, with only four residues having R_{ex} values greater than 3 s^{-1}. About one half of the assigned residues are mobile on the μs–ms time scale, resulting from conformational exchange, similar to the stromelysin/PNU-99533 complex.

Stromelysin/PNU-142372 complex

The overall correlation time of the complex was initially estimated from the R_2/R_1 ratio, 12.73 ± 1.96, to be 11.02 ± 0.92 ns and determined to be 10.83 ± 0.05 ns from the final analysis. The extracted model-free dynamic parameters are shown in Figure 3. The average S^2 value of the backbone ^{15}N nuclear spins is 0.86. Values of S^2 for the backbone nitrogen atoms have the following distribution: 10 residues have S^2 values less than 0.80, 79 residues have S^2 values between 0.80 and 0.90, and 56 residues have S^2 values greater than 0.90. Twenty-six residues required non-zero τ_e for an adequate fit and only six residues had their τ_e values obtained from the use of model 5. Sixty residues were determined to have non-zero R_{ex}, with two having R_{ex} values less than 1 s^{-1}. The mean R_{ex} value is 1.96 ± 0.85 s^{-1}, with seven residues having R_{ex} values greater than 3 s^{-1}.

Discussion

The changes of backbone and side chain dynamics of several proteins upon ligand binding have been studied using ^{13}C (Nicholson et al., 1992; Zhao et al., 1996), ^{15}N (Akke et al., 1993; Cheng et al., 1994; Farrow et al., 1994; Rischel et al., 1994; Epstein et al., 1995; Stivers et al., 1996; Yu et al., 1996; Hodsdon et al., 1997; Olejniczak et al., 1997) and ^{2}H-based (Kay et al., 1996) NMR spin relaxation experiments. Results from these studies have indicated that ligand binding induces a localized restriction of side chain and backbone motion near the ligand binding site. Unfortunately, the dynamics of apo-stromelysin could not be fully characterized because the ^{1}H-^{15}N HSQC spectrum is that characteristic of a partially unstructured protein undergoing conformational exchange and was not amenable to sequence-specific assignments. Instead, we have compared the dynamics of stromelysin complexed to ligands that bind in the S_1-S_3 (left) and S_1'-S_3' (right) regions of the active site. Dynamics measurements for the empty side of the active site in a given complex provide the basis to understand ligand-induced changes in active site dynamics. Some caution must be exercised when using this type of comparison since it is assumed that the S_1-S_3 and S_1'-S_3' subsites are independent and that ligand binding to one subsite does not affect the dynamics of the unoccupied site.

For most residues in the three complexes, the order parameters representing the relative amplitude of internal motion are greater than 0.8, indicating that the backbone internal motions of these residues on the picosecond time scale are highly restricted. A number of residues in each complex were found to have extremely restricted backbone internal motions with $S^2 > 0.90$. The relatively high S^2 values observed for the three stromelysin/inhibitor complexes is consistent with what has been reported for the related matrix metalloproteinase collagenase (Moy et al., 1997), and may be a general feature of this class of proteins.

With the exception of residues 150–155 described below, a ligand-related pattern for residues which have conformational flexibilities over the μs–ms time scale, as indicated by R_{ex}, was not well established, since residues determined to have non-zero R_{ex} values are distributed throughout the structure. Interpretation of R_{ex} values was complicated somewhat because contributions can arise from different sources such as the slow conformational exchange of the residue itself or changes in the chemical environment as a
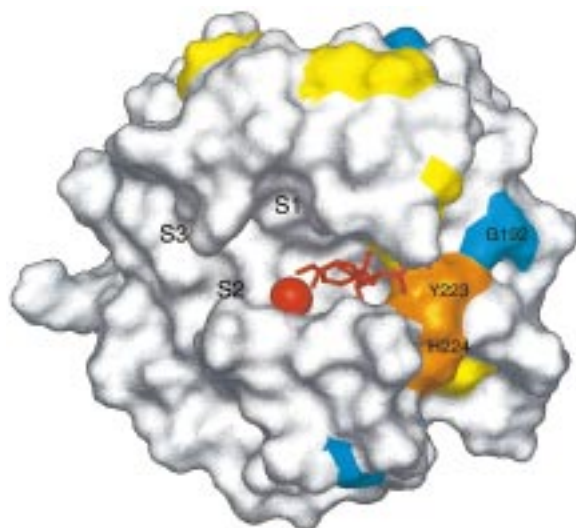
Figure 4. Accessible surface representation of the stromelysin/PNU-99533 complex active site face. Key residues discussed in the text and the empty S_1-S_3 subsites are labeled. The catalytic zinc atom and PNU-99533 are shown in red. Residues with S^2 values decreased by ≥ 0.1 in this complex compared to the stromelysin/PNU-107859 complex are shown in yellow. Residues with S^2 values increased by ≥ 0.1 in this complex compared to the stromelysin/PNU-107859 complex are shown in blue. Active-site residues whose $^1H^N$ resonances are broadened beyond detection in the stromelysin/PNU-107859 complex but not in this complex are shown in orange.

result of motion of vicinal residues or an element of secondary structure. One could speculate that the non-zero R_{ex} values may arise from a continuation of conformational exchange processes observed in apo-stromelysin that are not completely eliminated upon ligand binding.

Different dynamics profiles were observed for stromelysin complexed with chemically distinct ligands, as illustrated in Figure 4. The average order parameter for the 17 residues in the S_1-S_3 subsites within 5 Å of the thiadiazole ligands is 0.86 when the hydroxamate ligand PNU-99533 is bound. This compares to average order parameters of 0.88 and 0.89 for the thiadiazole ligands PNU-107859 and PNU-142372, respectively, suggesting that the S_1-S_3 subsites are only slightly disordered in the absence of interactions with ligand. The difference is greater for residues 151–155, which have an average order parameter of 0.75 in the stromelysin/PNU-99533 complex. This is approximately 0.1 less than either thiadiazole-containing complex, suggesting that this loop is reasonably mobile when lacking interactions between ligand and the tyrosine-155 side chain.
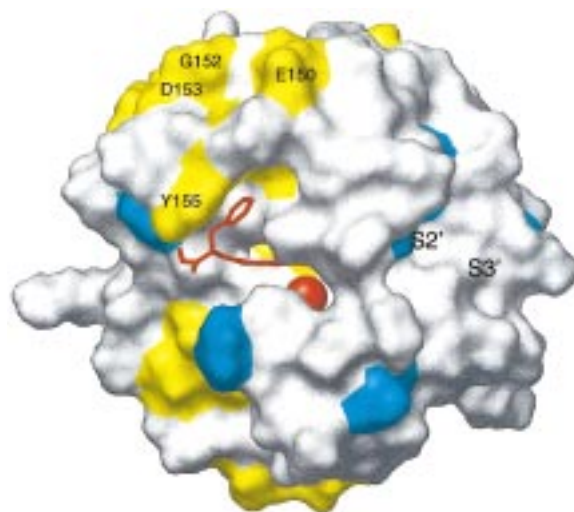
Figure 5. Accessible surface representation of the stromelysin/PNU-107859 complex active site face. Residues clustered in the 150–155 loop and the empty S_2' and S_3' subsites are labeled (the S_1' subsite is obscured). The catalytic zinc atom and PNU-107859 are shown in red. Residues with non-zero R_{ex} values in this complex but not in the stromelysin/PNU-142372 complex are shown in yellow. Residues with non-zero R_{ex} values in the stromelysin/PNU-142372 complex but not in this complex are shown in blue.

Residues 161–167, 197–198, 201–202, 205, 211 and 218-224 are within 5 Å of bound PNU-99533. The average order parameter for these residues in the stromelysin/PNU-99533 complex is 0.86. Interestingly, the average order parameters for these same residues in the stromelysin/PNU-107859 and stromelysin/PNU-142372 complexes are 0.88 and 0.89, respectively. However, these numbers are misleading since the order parameters for residues 223 and 224 are not included in the averages for the stromelysin/PNU-107859 and stromelysin/PNU-142372 complexes. The amide resonances of residues 223 and 224 were unassignable in these two complexes presumably because of line broadening. This suggests that residues 223 and 224, which as shown in Figure 4 form part of a flap at the bottom of the S_1'-S_3' binding site, are disordered in the absence of interactions with ligand. Additionally, residues 191 and 192, which comprise the end of a flap at the top of the S_1'-S_3' binding site, have order parameters that are reduced by about 0.3 in the thiadiazole complexes for which their values have been determined compared to their values in the stromelysin/PNU-99533 complex.

The S_1'-S_3' subsite residues that were broadened beyond detection or had low order parameters in the stromelysin/PNU-107859 and stromelysin/PNU-

142372 complexes were characterized by restricted internal motion in the stromelysin/PNU-99533 complex. The significant changes in the mobility of residues 191–192 and 223–224 are an indication that the S_1'-S_3' subsite of the stromelysin active site is flexible in the absence of interactions with ligand, but adopts a rigid conformation in the presence of ligand recognition interactions. A hydrogen bond formed between the histidine-224 amide proton and a carbonyl group in PNU-99533 probably accounts for the dramatically reduced mobilities of residues 223–224 in the stromelysin/PNU-99533 complex compared to the stromelysin/thiadiazole complexes, where this interaction is absent.

Similar observations have been made for the related protein collagenase. In the absence of inhibitor, residues 138–144 (corresponding to residues 220–226 in stromelysin) were found to be disordered as defined by low order parameters (Moy et al., 1997) and minimal NOEs (Moy et al., 1998). These residues appear to be well ordered in collagenase/inhibitor complexes as defined by low crystallographic B-factors (Spurlino et al., 1994). However, NMR studies have indicated that residues 138–144 remain highly disordered in the presence of a hydroxamate-containing ligand, with only minimal interactions existing between these residues and the ligand (Moy et al., 1997). This contrasts with our observations of the stromelysin/PNU-99533 complex and may result from a fundamental difference between stromelysin and collagenase or from differences in how ligand binding affects the dynamics of the two proteins.

The decrease in mobility in the stromelysin/PNU-99533 S_1'-S_3' subsite is accompanied by increased backbone mobility of other residues. As shown in Figure 4, the yellow residues, indicative of increased flexibility, are on the surface of the protein and dispersed throughout the structure. The phenomenon of increased mobility of residues as a result of ligand binding has been observed by Stivers et al. (1996) in their dynamics study of free and inhibitor-bound 4-oxalocrotonate tautomerase, and by Kay et al. (1996) in their study of PLCC SH2 domain.

Similar dynamics profiles were observed for stromelysin complexed with chemically similar ligands. The binding of a ligand to a protein will rigidify the region around the binding site (if it is not already rigid in the absence of interactions with ligand) and results in restricted motions of residues involved. PNU-107859 and PNU-142372 have nearly identical structures, the only difference being that the phenyl ring is fully fluorinated for the latter. PNU-142372 is a more effective inhibitor of stromelysin, with K_i of 18 nM compared to a K_i of 710 nM for PNU-107859. From analysis of the available structural data of these two stromelysin/ligand complexes, residues 155–158, 163–169, 175, 201–202, 205 and 210–211 are within 5 Å of the ligand (Finzel et al., 1998; Stockman et al., 1998). The average order parameter of these residues is 0.89 for the stromelysin/PNU-142372 complex and 0.88 for the stromelysin/PNU-107859 complex.

Differences were observed, however, in the residues with non-zero R_{ex} values in the two thiadiazole ligand complexes. These differences are illustrated in Figure 5. In particular, a cluster of residues near the ligand aromatic ring binding pocket have non-zero R_{ex} values in the stromelysin/PNU-107859 complex, but not in the stromelysin/PNU-142372 complex.

PNU-142372 was made by replacing the aromatic hydrogen atoms of PNU-107859 with fluorine atoms. This substitution has the effect of reversing the quadrupole moment of the aromatic ring (Bovy et al., 1991). Consequently, the electrostatic interaction between the protein and the aromatic ring of PNU-142372 must be different from that of PNU-107859. As determined from X-ray crystallographic data (Finzel et al., 1998), the aromatic ring of PNU-142372 interacts with the aromatic ring of tyrosine-155 in a parallel-plate fashion. This type of interaction results because the quadrupole moments of the two aromatic rings are in opposite orientations (Bovy et al., 1991; Dougherty, 1996). In the stromelysin/PNU-107859 complex, the interaction between the tyrosine-155 and ligand aromatic groups is most likely a perpendicular-plate one, since the quadrupole moments of the two aromatic rings are in identical orientations. While such interactions impact the mobility of the aromatic rings of the ligands, they also influence the mobility of tyrosine-155 and nearby residues. It is thus interesting to note that residues 150, 152, 153 and 155 had non-zero R_{ex} values in the stromelysin/PNU-107859 complex but not in the stromelysin/PNU-142372 complex. It has been estimated from ^{19}F NMR data that the PNU-142372 aromatic ring-flip rate is approximately 100/s, while that for the PNU-107859 aromatic ring is greater than 25 000/s (Stockman et al., 1998). The difference is attributable to the different stacking interactions of the two ligand aromatic rings with the tyrosine-155 aromatic ring. The non-zero R_{ex} values in the stromelysin/PNU-107859 complex may arise from conformational fluctuations of residues

150–155 associated with ligand aromatic ring flipping. These fluctuations appear to be frozen out by the tighter parallel-plate interaction of the PNU-142372 and tyrosine-155 aromatic rings.

The dynamics data presented here complement thermodynamics information obtained from calorimetry measurements of ligand binding to stromelysin (Sarver et al., 1999). Calorimetry measurements indicated that ligand binding to the S_1-S_3 subsites is predominantly enthalpy driven, with probably minimal solvent displacement and configuration consolidation (Sarver et al., 1999). This agrees with the picture emerging from NMR dynamics, indicating that the S_1-S_3 subsites are relatively rigid in the absence of ligand and do not experience significant ligand-induced conformational changes. By contrast, calorimetry measurements indicated that ligand binding to the S_1'-S_3' subsites is both enthalpy and entropy driven, with probably both solvent displacement from and configurational consolidation in the active site occurring (Sarver et al., 1999). This agrees with the NMR dynamics data indicating that the S_1'-S_3' subsites experience a ligand-induced loss of flexibility.

The results presented here are relevant to structure-based design of inhibitors of stromelysin and other MMPs. Studies have shown that the binding properties of a variety of ligands to a protein can be explained by knowledge of intrinsic dynamics of the binding site of the protein without knowing the precise geometry of the binding site or the interaction energies involved (Morton and Matthews, 1995; Kay et al., 1996). Therefore, efforts to establish the flexibility or plasticity of binding sites will complement structural studies designed to resolve which regions of a protein are most important for providing binding specificity and affinity. By studying the dynamics of stromelysin complexed with PNU-99533, PNU-107859 and PNU-142372, it has been observed that the S_1-S_3 subsites of the stromelysin active site are relatively rigid even in the absence of interactions with ligand, thus determining binding specificity by discriminating between ligands of different shapes. By contrast, the S_1'-S_3' subsites are quite flexible in the absence of interactions with bound ligand, allowing structural rearrangements to accommodate the incoming binding substrate or inhibitor and to accommodate the binding of other proteins at the active site from the right side. Such information is very important in explaining why thiadiazole ligands that bind to stromelysin are poor inhibitors of collagenase: lack of structural conservation in the S_1-S_3 subsites cannot be compensated for by

residue rearrangement. The S_1-S_3 subsites are rigid and cannot accommodate a broad range of ligands. In order to find broadly active inhibitors of MMPs using stromelysin as a target protein, it would be better to avoid the specificity imposed by the S_1-S_3 subsites and concentrate instead on finding potent ligands that can be accommodated by the S_1'-S_3' subsites. However, if inhibitors specific for certain MMPs are desired, the S_1-S_3 subsites provide intriguing design opportunities. The flexibility of the S_1'-S_3' subsites may result from a lack of interactions with other domains of stromelysin, in particular the C-terminal hemopexin-like domain, that are absent in the construct used in this study. The flexibility may also result from the need for the enzyme to accommodate a range of protein substrates, and to be able to release the products of the cleavage following proteolysis. If the latter is actually the case, then this inherent flexibility provides opportunities that can be exploited in the design of broad coverage MMP inhibitors.

Acknowledgements

References

Abragam, A. (1961) *Principles of Nuclear Magnetism*, Clarendon Press, Oxford.
Akke, M., Skelton, N.J., Kördel, J., Palmer III, A.G. and Chazin, W.J. (1993) *Biochemistry,* **32**, 9832–9844.
Barbato, G., Ikura, M., Kay, L.E., Pastor, R.W. and Bax, A. (1992) *Biochemistry,* **31**, 5269–5278.
Bax, A. and Pochapsky, S.S. (1992) *J. Magn. Reson.*, **99**, 638–643.
Becker, J.W., Marcy, A.I., Rokosz, L.L., Axel, M.G., Burbaum, J.J., Fitzgerald, P.M.D., Cameron, P.M., Esser, C.K., Hagmann, W.K., Hermes, J.D. and Springer, J.P. (1995) *Protein Sci.*, **4**, 1966–1976.
Bloom, M., Reeves, L.W. and Wells, E.J. (1965) *J. Chem. Phys.*, **42**, 1615–1624.
Bovy, P.R., Getman, D.P., Matsoukas, J.M. and Moore, G.J. (1991) *Biochim. Biophys. Acta*, **1079**, 23–28.
Cawston, T.E. (1996) *Pharmacol. Ther.*, **70**, 163–182.
Cheng, J.-W., Lepre, C.A. and Moore, J.M. (1994) *Biochemistry*, **33**, 4093–4100.
Clore, G.M., Szabo, A., Bax, A., Kay, L.E., Driscoll, P.C. and Gronenborn, A.M. (1990) *J. Am. Chem. Soc.*, **112**, 4989–4991.

Dhanaraj, V., Ye, Q.Z., Johnson, L.L., Hupe, D.J., Ortwine, D.F., Dunbar Jr., J.B., Rubin, J.R., Pavlovsky, A., Humblet, C. and Blundell, T.L. (1996) *Structure*, **4**, 375–386.

Dickens, J.P., Donald, D.K., Kneen, G. and McKay, W.R. (1987) European Patent EP 214639.

Dougherty, D.A. (1996) *Science*, **271**, 163–168.

Epstein, D.M., Benkovic, S.J. and Wright, P.E. (1995) *Biochemistry*, **34**, 11037–11048.

Farrow, N.A., Muhandiram, R., Singer, A.U., Pascal, S.M., Kay, C.M., Gish, G., Shoelson, S.E., Pawson, T., Forman-Kay, J.D. and Kay, L.E. (1994) *Biochemistry*, **33**, 5984–6003.

Finzel, B.C., Baldwin, E.T., Bryant Jr., G.L., Hess, G.F., Trepod, C.M., Mott, J.E., Marshall, V.P., Petzold, G.L., Poorman, R.A., O'Sullivan, T.J., Schostarez, H.J. and Mitchell, M.A. (1998) *Protein Sci.*, **7**, 2118–2126.

Gooley, P.R., Johnson, B.A., Marcy, A.I., Cuca, G.C., Salowe, S.P., Hagmann, W.K., Esser, C.K. and Springer, J.P. (1993) *Biochemistry*, **32**, 13098–13108.

Gooley, P.R., O'Connell, J.F., Marcy, A.I., Cuca, G.C., Axel, M.G., Caldwell, C.G., Hagmann, W.K. and Becker, J.W. (1996) *J. Biomol. NMR*, **7**, 8–28.

Gooley, P.R., O'Connell, J.F., Marcy, A.I., Cuca, G.C., Salowe, S.P., Bush, B.L., Hermes, J.D., Esser, C.K., Hagmann, W.K., Springer, J.P. and Johnson, B.A. (1994) *Nat. Struct. Biol.*, **1**, 111–118.

Grzesiek, S. and Bax, A. (1993) *J. Am. Chem. Soc.*, **115**, 12594–12595.

Hodsdon, M.E. and Cistola, D.P. (1997) *Biochemistry*, **36**, 2278–2290.

Jacobsen, E.J., Mitchell, M.A., Hendges, S.K., Belonga, K.L., Skaletzky, L.L., Stelzer, L.S., Lindberg, T.J., Fritzen, E.L., Schostarez, H.J., O'Sullivan, T.J., Maggiora, L.L., Stuchly, C.W., Laborde, A.L., Kubicek, M.F., Poorman, R.A., Beck, J.M., Miller, H.R., Petzold, G.L., Scott, P.S., Truesdell, S.E., Wallace, T.L., Wilks, J.W., Fisher, C., Goodman, L., Kaytes, P.S., Ledbetter, S.R., Powers, E.A., Vogeli, G., Mott, J.E., Trepod, C.M., Staples, D.J., Baldwin, E.T. and Finzel, B.C. (1999) *J. Med. Chem.*, **42**, 1525–1536.

Kay, L.E., Muhandiram, D.R., Farrow, N.A., Aubin, Y. and Forman-Kay, J.D. (1996) *Biochemistry*, **35**, 361–368.

Kay, L.E., Torchia, D.A. and Bax, A. (1989) *Biochemistry*, **28**, 8972–8979.

Lipari, G. and Szabo, A. (1982a) *J. Am. Chem. Soc.*, **104**, 4546–4559.

Lipari, G. and Szabo, A. (1982b) *J. Am. Chem. Soc.*, **104**, 4559–4570.

MacDougall, J.R. and Matrisian, L.M. (1995) *Cancer Metastasis Rev.*, **14**, 351–362.

Mandel, A.M., Akke, M. and Palmer III, A.G. (1995) *J. Mol. Biol.*, **246**, 144–163.

Morton, A. and Matthews, B.W. (1995) *Biochemistry*, **34**, 8576–8588.

Moy, F.J., Chanda, P.K., Cosmi, S., Pisano, M.R., Urbano, C., Wilhelm, J. and Powers, R. (1998) *Biochemistry*, **37**, 1495–1504.

Moy, F.J., Pisano, M.R., Chanda, P.K., Urbano, C., Killar, L.M., Sung, M.-L. and Powers, R. (1997) *J. Biomol. NMR*, **10**, 9–19.

Nicholson, L.K., Kay, L.E., Baldisseri, D.M., Arango, J., Young, P.E., Bax, A. and Torchia, D.A. (1992) *Biochemistry*, **31**, 5253–5263.

Olejniczak, E.T., Zhou, M.M. and Fesik, S.W. (1997) *Biochemistry*, **36**, 4118–4124.

Palmer III, A.G., Rance, M. and Wright, P.E. (1991) *J. Am. Chem. Soc.*, **113**, 4371–4380.

Piotto, M., Saudek, M. and Sklenar, J. (1992) *J. Biomol. NMR*, **2**, 661–665.

Porter, J.R., Millican, T.A. and Morphy, J.R. (1995) *Exp. Opin. Ther. Pat.*, **5**, 1287–1296.

Rischel, C., Madsen, J.C., Andersen, K.V. and Poulsen, F.M. (1994) *Biochemistry*, **33**, 13997–14002.

Sarver, R.W., Yuan, P., Marshall, V.P., Petzold, G.L., Poorman, R.A., DeZwaan, J. and Stockman, B.J. (1999) *Biochim. Biophys. Acta*, in press.

Shaka, A.J., Keeler, J., Frenkiel, T. and Freeman, R. (1983) *J. Magn. Reson.*, **52**, 335–338.

Sklenar, V., Torchia, D.A. and Bax, A. (1987) *J. Magn. Reson.*, **73**, 375–379.

Spurlino, J.C., Smallwood, A.M., Carlton, D.D., Banks, T.M., Vavra, K.J., Johnson, J.S., Cook, E.R., Falvo, J., Wahl, R.C., Pulvino, T.A., Wendoloski, J.J. and Smith, D.L. (1994) *Protein Struct. Funct. Genet.*, **19**, 98–109.

Stivers, J.T., Abeygunawardana, C., Mildvan, A.S. and Whitman, C.P. (1996) *Biochemistry*, **35**, 16036–16047.

Stockman, B.J., Waldon, D.J., Gates, J.A., Scahill, T.A., Kloosterman, D.A., Mizsak, S.A., Jacobsen, E.J., Belonga, K.L., Mitchell, M.A., Mao, B., Petke, J.D., Kaytes, P.S., Goodman, L., E., Powers, E.A., Fisher, C., Ledbetter, S.R., Vogeli, G., Marshall, V.P., Petzold, G.L. and Poorman, R.A. (1998) *Protein Sci.*, **7**, 2281–2286.

Van Doren, S.R., Kurochkin, A.V., Hu, W., Ye, Q.-Z., Johnson, L.L., Hupe, D.J. and Zuiderweg, E.R.P. (1995) *Protein Sci.*, **4**, 2487–2498.

Van Doren, S.R., Kurochkin, A.V., Ye, Q.-Z., Johnson, L.L., Hupe, D.J. and Zuiderweg, E.R.P. (1993) *Biochemistry*, **32**, 13109–13122.

Wojtowicz-Praga, S.M., Dickson, R.B. and Hawkins, M.J. (1997) *Invest. New Drugs*, **15**, 61–75.

Yu, L., Zhu, C.-X., Tse-Dinh, Y.-C. and Fesik, S.W. (1996) *Biochemistry*, **35**, 9661–9666.

Zask, A., Levin, J.I., Killar, L.M. and Skotnicki. J.S. (1996) *Curr. Pharm. Des.*, **2**, 624–661.

Zhao, Q., Abeygunawardana, C. and Mildvan, A.S. (1996) *Biochemistry*, **35**, 1525–1532.